


## Article

# A Neural Network-Based Flame Structure Feature Extraction Method for the Lean Blowout Recognition

Puti Yan <sup>1</sup>, Zhen Cao <sup>1,2,3,\*</sup>, Jiangbo Peng <sup>1,2</sup>, Chaobo Yang <sup>1,2</sup>, Xin Yu <sup>1,2</sup> , Penghua Qiu <sup>3</sup>, Shanchun Zhang <sup>1,2</sup>, Minghong Han <sup>1,2</sup>, Wenbei Liu <sup>1,2</sup> and Zuo Jiang <sup>4</sup>

<sup>1</sup> School of Astronautics, Harbin Institute of Technology, Harbin 150001, China; classicypt1230@163.com (P.Y.); pengjiangbo@hit.edu.cn (J.P.); yangchaobo@hit.edu.cn (C.Y.); yuxin0306@hit.edu.cn (X.Y.); zsc19931225@163.com (S.Z.); minghong\_h@163.com (M.H.); liuwenbei@stu.hit.edu.cn (W.L.)

<sup>2</sup> National Key Laboratory of Science and Technology on Tunable Laser, Harbin Institute of Technology, Harbin 150001, China

<sup>3</sup> Postdoctoral Research Station of Power Engineering and Engineering Thermophysics, Harbin Institute of Technology, Harbin 150001, China; qiuph@hit.edu.cn

<sup>4</sup> Research Center of Intelligent Systems, China Aerospace Science and Industry Corporation, Beijing 100048, China; jiangzuomove@icloud.com

\* Correspondence: caozhen1995@hit.edu.cn; Tel.: +86-18845151314

**Abstract:** A flame's structural feature is a crucial parameter required to comprehensively understand the interaction between turbulence and flames. The generation and evolution processes of the structure feature have rarely been investigated in lean blowout (LBO) flame instability states. Hence, to understand the precursor features of the LBO flame, this work employed high-speed OH-PLIF measurements to acquire time-series LBO flame images and developed a novel feature extraction method based on a deep neural network to quantify the LBO features in real time. Meanwhile, we proposed a deep neural network segmentation method based on a tri-map called the Fire-MatteFormer, and conducted a statistical analysis on flame surface features, primarily holes. The statistical analysis results determined the relationship between the life cycle of holes (from generation to disappearance) and their area, perimeter, and total number. The trained Fire-MatteFormer model was found to represent a viable method for determining flame features in the detection of incipient LBO instability conditions. Overall, the model shows significant promise in ascertaining local flame structure features.

**Keywords:** lean blowout; high-speed OH-PLIF; neural network; flame structure; feature extraction



**Citation:** Yan, P.; Cao, Z.; Peng, J.; Yang, C.; Yu, X.; Qiu, P.; Zhang, S.; Han, M.; Liu, W.; Jiang, Z. A Neural Network-Based Flame Structure Feature Extraction Method for the Lean Blowout Recognition. *Aerospace* **2024**, *11*, 57. <https://doi.org/10.3390/aerospace11010057>

Academic Editors: Yu Guan and Jingxuan Li

Received: 4 November 2023

Revised: 31 December 2023

Accepted: 2 January 2024

Published: 7 January 2024



**Copyright:** © 2024 by the authors. Licensee MDPI, Basel, Switzerland. This article is an open access article distributed under the terms and conditions of the Creative Commons Attribution (CC BY) license (<https://creativecommons.org/licenses/by/4.0/>).

## 1. Introduction

A lean premixed swirl flame is the main combustion form in a low-emission gas-turbine engine or aero-engine, which generates recirculation zones to stabilize the flame structure [1,2]. In the context of reducing NO<sub>x</sub> emission, the swirl flame easily becomes extinct due to very low equivalence ratio levels. Meanwhile, the extinction events and vortex breakdown become more likely to occur once the lean limit is reached, exacerbating the complexity of the interaction between flow and combustion [3–5]. The investigation of the flame structure feature characterizing the flame evolution process is of great significance for understanding dynamic behaviors and recognizing the flame state. Lean blowout (LBO) is a common hot issue in swirl-stabilized combustors. When flame approaches LBO, it becomes unstable; thus, mastering LBO flame behavior, such as flame structure evolution, is extremely important for the efficient, reliable, and safe operation of a gas-turbine engine or aero-engine. Recently, the investigation of LBO characteristics has received widespread attention, especially regarding flame feature investigation at near-LBO condition. However, it is very challenging to identify the LBO limit due to strongly coupled and unsteady processes [6,7]. Reliable flame features are always essential for the early identification of

LBO and understanding of the instability mechanism, which are significant in the design of reliable and safe gas turbine combustors. Vortex fragmentation can lead to flame surface rupture and local flameout, generating abundant local structural features, such as the flame hole. Hole features can reflect the details of the interaction between turbulence and flames to some extent. Many findings in the literature have found a connection between local structure features and flame characteristics [8,9], but further research is needed to determine whether it can be used to analyze combustion states. The generation and evolution of the local structure feature are crucial in the investigation of flame stability and LBO prediction methods, which may serve as a precursor feature for LBO state recognition [10].

High-speed planar laser-induced fluorescence and chemiluminescence imaging are most frequently used to obtain the spectral information regarding intermediate combustion components (such as CH and OH groups). In addition, the multi-dimensional flame dynamic information of the combustion field can be obtained to conduct an in-depth analysis of combustion characteristics [11,12]. For example, high-speed chemiluminescence imaging has been developed and applied to analyze the unstable process of swirling flame extinction. However, the combustion information obtained using the chemiluminescence imaging method has the path integration characteristics, which makes it difficult to obtain high-resolution flame fine structure information. Furthermore, planar laser-induced fluorescence of OH radical (OH-PLIF) was frequently used to obtain the flame location and local flame structure with high spatial resolution. Taamallah et al. [13] investigated the premixed swirl flame macrostructures in different stabilization modes, and found the presence of a vortex structure along the inner shear layer zone by means of the OH-PLIF technique. However, the evolution process could not be carried out due to the lower acquisition speed of 10 Hz. Zhang et al. [14] used simultaneous 10 kHz PLIF and stereoscopic particle image velocimetry (S-PIV) to study local feature dynamic behavior, including the processing vortex core, and the growth or decay was quantified as an instability feature of the flow. Furthermore, the local structure features and effects on flame dynamic and heat-release fluctuation were also investigated by Wang et al. [15]. Skiba et al. [16] investigated the effects of large eddies on turbulent premixed flame structures using high-speed multi-species PLIF and PIV, and identified two common flow-flame events in the PLIF-PIV movies, expressing the interactions between turbulent structures (eddies) and premixed flame fronts. These results can confirm the roles of local flame structures such as holes. Therefore, the local flame structure detail was closely related to the degree of flow-flame interaction, which can be used as an indicator to study the combustion condition. In addition, there are a lack of efficient local feature extraction methods, resulting in very limited features that can be used to analyze the lean burn extinction process of swirling flames.

Relevant research aimed at the cross-disciplinary area of energy and artificial intelligence has obtained many meaningful results, for example, reconstructing PLIF images using chemiluminescence images [17], and improving the resolution ratio of spatiotemporal evolution based on the frame interpolation method and an accurate prediction of the combustion state [18]. Aiming to investigate local flame structure features, aside from using traditional methods such as flame geometric and intensity features, researchers have conducted extensive work on the intelligent processing of flame images and pattern recognition of combustion field images, especially the combination of big data, machine learning, and artificial intelligence [19]. To improve the interpretability of the model and reduce its complexity, the quantified flame structure features should be extracted and investigated instead of raw images. In order to obtain the image features most directly related to the combustion state and establish a mapping relationship between the image features and combustion state, many structure feature extraction and analysis methods have been developed. In our recent works, flame area and moment features have been used to investigate the near-LBO flame dynamics. The heat-release frequencies and dominant oscillation modes were obtained to demonstrate the oscillation characteristics of the near-LBO flame [20]. In the above-mentioned study, a flame hole structure from a turbulent flame front was found, but whether it can be used as a novel flame feature requires subse-

quent research. Meanwhile, basic image features such as flame area, flame circumference, and vertical range, among others, were also used to establish the scramjet/ramjet model classifier by means of K-nearest neighbor (KNN) [21]. Other potential features need to be explored further. Hasti et al. [22] proposed a data-driven method based on support vector machine (SVM) to identify the critical flame location of the LBO flame. The temperature and OH mass fraction from the large eddy simulation were used as training data to establish the machine learning model. The flame root region was found to have significant advantages in characterizing the critical flame location. Roncancio et al. [23] combined OH-PLIF images and a convolutional neural network (CNN) model to classify the burned and unburned turbulent media. The local flame structure features, including the pockets or islands, were extracted and reduced the computational time significantly. Additionally, seeking a quantifiable new feature is highly beneficial for flame condition recognition.

In this paper, the properties of flame images are further explored. In order to accurately extract the flame structure feature from PLIF images, it is necessary to use image segmentation algorithms. Although some simple computer vision algorithms like improved threshold methods can be effective, these algorithms need to carefully adjust each parameter of the algorithm according to each combustion scene, and they are not robust to scene changes. In order to achieve more accurate segmentation, image matting has been applied as a representative of fine subject segmentation technology. For example, Xu et al. [24] first proposed a two-stage neural network architecture for a tri-map based on image matting and then released the Composition-1K dataset. MatteFormer [25] utilizes the most advanced transformer architecture and enhances the global information of the network through prior tokens. Although these methods have made great progress, they are more commonly used in the foreground segmentation of natural images or portraits. At present, there is no work in the image matting area that can be directly used in the analysis of flame images. The tri-map-based segmentation method is suitable for the analysis of the scene in this paper, but it cannot be directly applied to flame images. The current work on deep learning-based computer vision and a flame combustion image mainly analyzes the flame properties in the natural image, and it lacks an understanding of the internal mechanism and interaction of the flame. Therefore, it is reasonable to design a framework to introduce tri-map-based flame segmentation into the analysis of flame images.

Most prior LBO studies have observed that significant changes in flame structure features exist within the LBO flame. However, to our knowledge, the limited LBO features are extracted and analyzed due to the lack of experimental data and an efficient flame feature extraction method. The few LBO features from available experimental data were reported, especially the local flame structure features for the investigation of LBO recognition and combustion characteristics. In this paper, we developed a quantified flame structure feature extraction neural network-based method to establish the correlation with the LBO state. In response to the demands of acquisition and analysis for high-resolution local flame structure information in LBO flames, this work explores a flame structure feature for LBO recognition based on high-speed OH-PLIF images. By recognizing the gaps in current methodologies, particularly in combining the deep neural networks and available flame images, this study meticulously analyzes engine flame images to extract the whirls of flames by harnessing the power of the self-attention-based transformer architecture. Furthermore, a novel spatiotemporal matching analysis framework is introduced to analyze the extracted results. To discern and document the statistical patterns inherent in the flame combustion process, this study provides a more in-depth understanding of flame combustion dynamics, offering invaluable insights and guidance in the study of combustion patterns. Finally, we will delve deep into the intricacies of flame image properties and the application of advanced image segmentation techniques, culminating in a comprehensive framework that combines the strength of computer vision, deep learning, and intricate flame combustion mechanisms. Based on the above issues, this work aims to develop two high-speed PLIF diagnostic techniques, including the burst mode (10 kHz repetition rate) and continuous mode (1 kHz repetition rate) to obtain the experimental data of LBO flame

evolution. To understand the lean blowout process and further analyze the combustion instability, an efficient feature extraction and analysis method were presented, and some significant LBO evolution parameters were obtained, including the relationship between the life cycle of hole structures (from generation to disappearance) and their area, perimeter, and total number to derive the evolution time. It is important to note that this study aims to extract the hole features for LBO recognition instead of predicting them. However, this data analysis method and flame features can provide new insights for flame blowout prediction in the future.

## 2. Methodology

### 2.1. Experiment Details

An aero-engine model combustor with an optical window was used for the investigation of the LBO flame in this paper. The swirl-stabilized burner structure was similar to the dual-swirl burner model of the German Aerospace Center (DLR), which can be a typical research object of swirl flow structure and dynamics. The schematic of the dual-swirl burner setup has been reported in our recent work [20]. The angle of the primary swirler is  $45^\circ$  with a swirl number of 0.11. The angle of the secondary swirler is  $60^\circ$  with a swirl number of 1.79. Methane fuel is transported in three streams to the combustion chamber, and the inlet is connected to the fuel nozzle through six inclined holes, with an inner diameter of 15.6 mm and an outer diameter of 16.4 mm. By changing the equivalent ratio of fuel, two typical flame conditions are obtained, including stabilization ( $\varphi = 0.4$ ) and near-LBO ( $\varphi = 0.1$ ). As for the optical diagnostic techniques, the high-speed OH-PLIF technique with 10 kHz and 1 kHz repetition rates was used to obtain a large amount of flame data representing the LBO flame evolution. The acquisition speed for the PLIF system refers to the frame frequency of images. The laser pulse width is 10 ns, which is sufficient to freeze the reaction flow field with high temporal resolution. In the 1 kHz PLIF mode, the CMOS array was  $1856 \times 970$  pixels, corresponding to a  $70 \text{ mm} \times 50 \text{ mm}$  imaging field of view, giving a spatial resolution of about  $67 \mu\text{m}$  per pixel. In the 10 kHz PLIF mode, the CMOS array was  $1000 \times 1000$  pixels, and the spatial resolution was about  $75 \mu\text{m}$  per pixel.

For the extraction of structure features, the extraction and analysis model of hole structure was trained and validated based on 10 kHz and 1 kHz PLIF image data, respectively. Two OH-PLIF technique working modes were used, including the burst mode of short duration and continuous working mode in the present study. OH fluorescence was facilitated by exciting the Q1(8) transitions in the (0,0) band of the  $A^2\Sigma^+ - X^2\Pi$  system at 283.553 nm via a frequency-doubled dye laser (Sirah Credo, with Rhodamine 6G) pumped by a self-researched high-speed Nd: YAG laser. The ultraviolet laser pulse was used to excite OH radicals, corresponding to an energy of 1.5 mJ at 1 kHz, and 1.8 mJ at 10 kHz. The imaging field of view was  $70 \text{ mm} \times 50 \text{ mm}$ , giving a spatial resolution of about  $67 \mu\text{m}$  per pixel. The laser sheet thickness was nearly  $200 \mu\text{m}$  to allow high-spatial resolution measurement of the flame structure. Fluorescence was obtained using a high-speed intensified CMOS camera coupled with the combination of Semrock 315 nm/15 nm and Schott UG11. The CMOS array was  $1856 \times 970$  pixels with an operation rate at 1 kHz and  $1000 \times 1000$  pixels at 10 kHz. On the one hand, we used a 10 kHz burst-mode PLIF technique to analyze the characteristics of local hole development in small time scales ( $\sim$ millisecond). In this mode, the single burst train contains 30 pulses with a minimum pulse interval of  $100 \mu\text{s}$ . The fine-hole structure evolution can be obtained to train the feature data extraction model. On the other hand, the continuous 1 kHz OH-PLIF mode was used to obtain a large number of images under a continuous flame evolution process, for example, 3000 pairs of images to validate the deep neural network segmentation method. Furthermore, a statistical analysis of structure features was adopted to assess the relationship between combustion conditions, such as stabilization or near-LBO condition. In this paper, a data model for the extraction and analysis of swirl structure features is described in detail. This article, as a continuation of our research work on LBO flame characteristics, aims to elucidate a deeper understand-

ing of the near-LBO condition and provide an effective structure feature parameter and model for LBO recognition and online prediction.

## 2.2. Neural Network for Feature Extraction

The framework proposed in this paper is shown in Figure 1. For the input flame image, this paper first generates its tri-map. Then, the flame image and its tri-map are sent to Flame-MatteFormer to segment the main outline of the flame. After that, this paper designs a series of post-processing processes, including main contour correction, edge compensation, global instance extraction, and instance feature analysis. The purpose of these steps is to reduce the noise of the main contour, extract the hole instances of a single image, and analyze its features. After that, this paper designs a spatio-temporal matching and analysis algorithm to apply a global spatio-temporal analysis of the hole extraction results of all frames. This proposal introduces a neural network tri-map-based segmentation method. The tri-maps are fed to the neural network together with the original flame images to obtain the main contour in the flame image. Through post-processing, the flame contour is further refined, all closed contours are extracted, and noise is filtered. After feature extraction, the temporal characteristics of the hole are analyzed to obtain the specific number of the hole feature, as well as the total number and the life cycle of each hole in the frame. Finally, over time, the statistical analysis results are obtained.

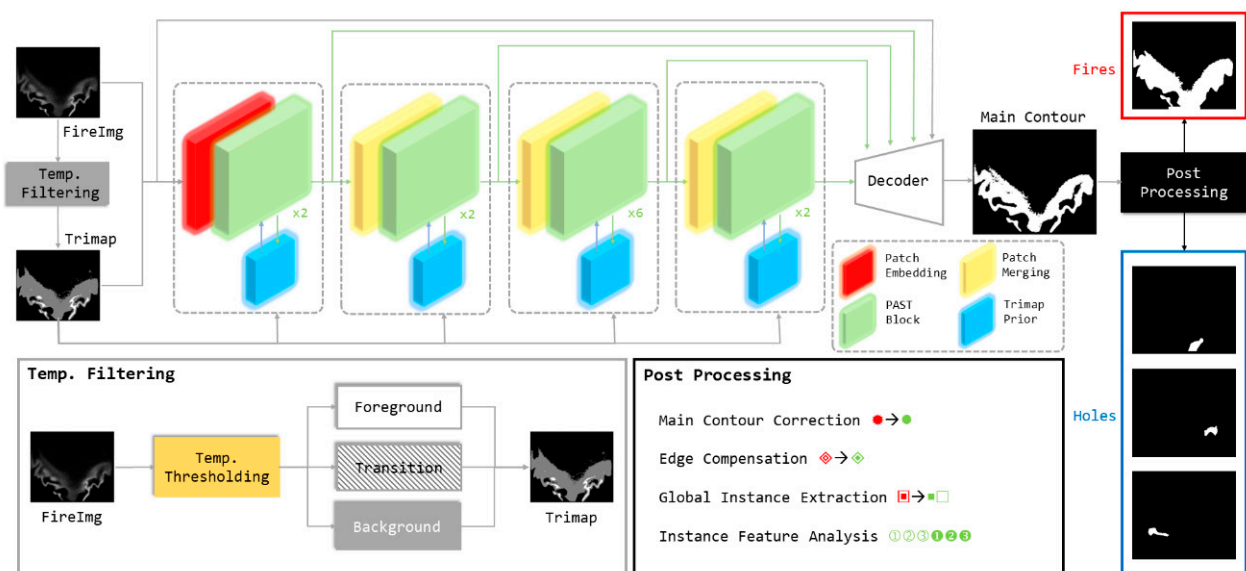


**Figure 1.** Schematic representation showing the generating process of feature extraction based on the neural network.

For the extraction of the main contour in the swirling flame, a neural network tri-map-based segmentation method is introduced. The tri-map is a concept originally introduced in the field of image matting [26–28], where the goal is to better segment the foreground from various backgrounds with priors. The tri-map is obtained by setting the threshold of the background and flame to be relatively extreme values, while the regions of other values are classified into the uncertain region. Using this definition, the network’s learning objective is to generate the correct foreground segmentation map given an input image  $I$  and a tri-map  $T$ . In this paper, we introduce the concept of the tri-map and modify the definition to better fit the characteristics of the fire flame image. The tri-map  $T_i$  for the  $i$ -th flame image can be obtained by

$$T_i(x, y) = \begin{cases} 0, & X_i < t_1 \\ 1, & X_i > t_2 \\ 0.5, & \text{else} \end{cases} \quad (1)$$

where  $t_1$  and  $t_2$  are threshold values for the determined background and the flame. We can set the threshold to be strict so that most areas are classified as transition areas. Then, the neural network learns to combine density and spatial information to automatically determine the location of large transition areas. Compared to the threshold methods that eliminate spatial information through statistics, the tri-map retains spatial relationships, allowing the network to determine the flame or hole locations through brightness and the context around it. Meanwhile, the internal brightness of the hole in the flame image is sometimes bright and dark. A fixed threshold will lead to confusion as the brighter holes are easily divided into the foreground, and vice versa. In this paper, we modified the deep image matting method MatteFormer [25] to satisfy the requirements of segmenting flame images, and we called the modified network Flame-MatteFormer.

MatteFormer adapts the popular transformer architecture [29] to achieve the task of foreground segmentation by enhancing contextual modeling through self-attention, which outperforms traditional methods based on convolutional neural networks in terms of global perception. Meanwhile, its window-based processing preserves enough local information. The MatteFormer with self-attention is well suited for the joint processing of global and local information, which is crucial for segmenting flame contours.

In addition, the self-attention can be obtained as follows:

$$\text{Attention}(Q, K, V) = \text{softmax}\left(\frac{QK^T}{\sqrt{d_k}}\right)V \quad (2)$$

where  $Q, K, V$  are obtained by transforming  $X$  with learnable parameters. The key to the attention mechanism is to generate the weights based on different inputs and then weigh the input values. The self-attention mechanism is different in that the weights and values are generated by the same input.

The MatteFormer first defines the prior-token, which represents the global context feature of the tri-map. In Flame-MatteFormer, this represents the global information such as the area of the flame, background, or transition regions. The first prior token of the network corresponds to the specific number of pixels in the flame, background, or transition regions. These prior-tokens are used as global priors and participate in the attention mechanism of each basic module. The method for generating the prior-tokens is as follows:

$$p^q = \frac{1}{N_q} \sum_{i=1}^N r_i^q \cdot z_i, \quad q \in \{\text{fg}, \text{bg}, \text{tr}\} \quad (3)$$

where  $q$  is one of the foreground (flame), background, and transition regions,  $N_q$  is the area of that region,  $N$  is the total space,  $r_i^q$  indicates whether the region is part of  $q$ , and  $z_i$  is the density of the region.

Secondly, the MatteFormer consists of Prior-Attention Swin Transformer (PAST) blocks, which are based on Swin Transformer blocks [30] but introduce the Prior-Attention-Weighted Self-Attention (PA-WSA) layer. In this layer, self-attention uses not only spatial information but also prior-tokens to calculate attention. In this way, each basic module considers not only the local spatial information but also the global statistical information of the flame. The expression of PA-WSA is as follows:

$$\text{Attention}(Q, K, V) = \text{softmax}\left(QK^T \cdot s + B\right)V \quad (4)$$

where  $s$  is the proportion factor, which is the same as the  $\frac{1}{\sqrt{d_k}}$  in the original attention equation. The modification in this paper is the addition of the positional offset  $B$ , which is used to adjust the self-attention further. In addition, Matteformer also introduces prior-memory, which stores the prior-tokens generated by each block. This allows the block to reuse the tokens generated from the previous block, which strengthens the global information by reminding the network of known regions' statistics. The working mechanism of this part is further illustrated in Figure 2.

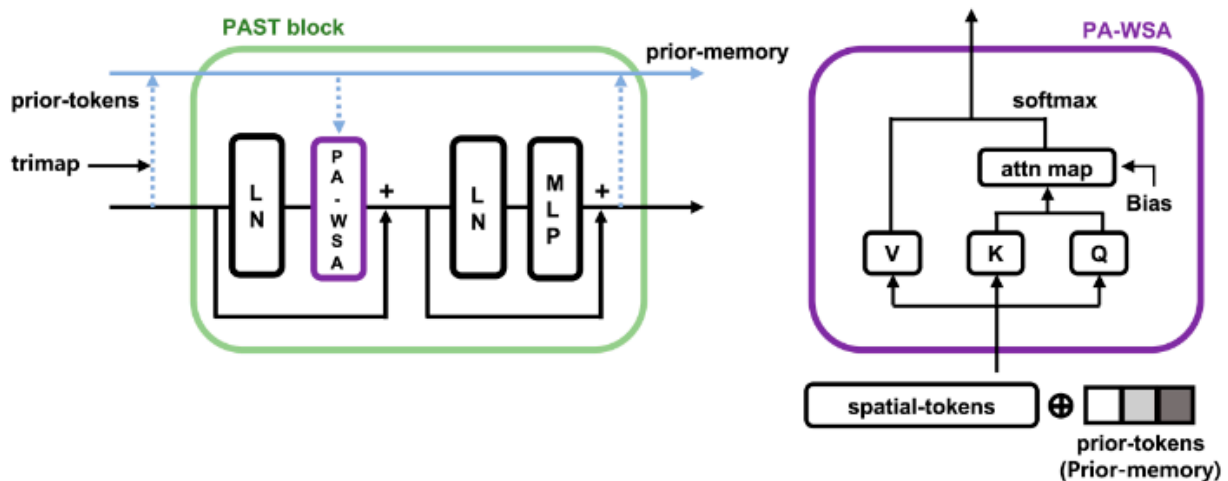


**Figure 2.** The structure diagram of the Prior-Attention Swin Transformer (PAST) block and Prior-Attention-Weighted Self-Attention (PA-WSA) layer [25].

Finally, the extracted main contours are further refined through four different post-processing steps. The first step is the main contour correction. This step utilizes a  $5 \times 5$  morphology kernel to perform close and open operations on the extracted contour to eliminate small holes and connections. The second step is the edge compensation. This step fills in gaps in the flames on both sides by setting a fixed proportion of the brightness ratio to detect potential holes and seal the outlines for better analysis. The third step is the global instance extraction. The extraction algorithm used is the Suzuki algorithm [31]. As shown in Figure 1, we extract all significant contours of the flame. Finally, the instance feature analysis step can be conducted. This step aims to differentiate noise, flames, and holes. The method first separates noise by identifying the size of the area. Then, the flames and holes are separated by calculating the average brightness within the area. If the average brightness is small, it is considered a hole feature; otherwise, it is considered a flame.

Overall, the proposed Flame-MatteFormer first divides the input flame image into 16 patches, where each patch is processed and projected separately, and the projected feature expansion is modeled as a sequence feature to be provided for subsequent processing. At each stage, the network structure consists of patch embedding or patch merging and several PAST blocks. The function of patch embedding is to apply feature projection to the sequence features, while the function of patch merging is to rearrange the sequence features to increase the feature dimension and reduce the size of the feature maps. Following this, the sequence features are fed into the PAST block for processing, and the details of this section can be found in the methodology introduction section above. At the end of each stage, the sequence features can recover the spatial representation, which is similar to the feature map; thus, the feature map obtained via transformer-based methods can be used for fine-grained spatial tasks. Finally, the output feature maps of different stages are collected and sent to the decoder, which is a convolution neural network used to recover the foreground segmentation results from input feature maps. The concrete structure is the combination of a convolution block with residual connection and nearest neighbor upsampling, and the feature is gradually restored to the size of the original image.

In the process of network training, the network initializes with the MatteFormer trained on the Composition-1K dataset. Following this, the network is fine-tuned on the collected LBO images. A total of 2000 LBO images are collected, including 1000 in a stable state and 1000 in an unstable state, of which 700 are used for training and 300 for testing. During the fine tuning process, the batch size is set to 20. The learning rate is initialized to 0.0002. The Adam optimizer is used, and the training time is 20 k iterations. Finally, the best metric on the test set is  $MSE = 0.021$ .

### 3. Results

#### 3.1. Validation of Fire-MatteFormer Method

In this section, the Fire-MatteFormer processing results are qualitatively and quantitatively assessed, considering the temporal and spatial correlations of hole structure evolution. Based on the high-speed OH-PLIF images obtained in the experiments, the hole structure features were extracted in the flame image captured at each time point, as shown in Figure 3. The temporal relationship can be analyzed to gain a comprehensive understanding of the process from the generation to extinction of hole structures. The specific operation process is as follows: Firstly, for the first image of time-resolved OH-PLIF sequences, we consider all the holes as being newly formed and record their size and center point simultaneously. For subsequent image frames, the holes are extracted and similar markings as above are conducted. Then, the spatial relationship between the two sets of center points are calculated based on the previous frame's hole and the current frame's hole using the distance-matching principle. The tracking of identical hole features is of great significance in analyzing the dynamic evolution of these holes over time, and further investigating the interaction between turbulence and flame structure. After obtaining the matched relationship, we first traverse the holes in the previous frame. If there is no hole in the current frame that matches the corresponding hole in the previous frame, it means that the corresponding hole has disappeared; if there is a hole in the current frame that matches one of the holes in the previous frame, we will adjust the number of the corresponding hole in the current frame to the number of the hole in the previous frame; if there are multiple holes in the current frame that match the holes in the previous frame, we need to examine the relationship between the area of each hole and the areas of the corresponding holes. If the two areas are close, it means that the hole has split into multiple holes, and each corresponding hole will be assigned a new number. If the areas are not close, it means that there are multiple matching errors, so the closest hole will be assigned a new number, and the other holes will be assigned new numbers.

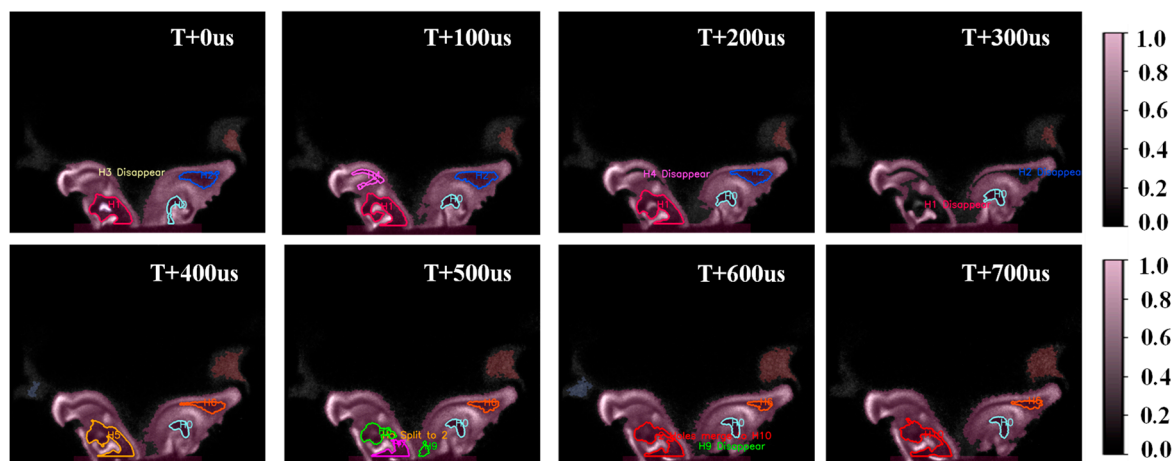


**Figure 3.** Time-resolved OH-PLIF images with a time interval of 100  $\mu$ s. The extracted hole structure was marked based on the Fire-MatteFormer method. The color key represents the value of the pixel, where white represents high values and black represents low values.

Firstly, we explore the matching relationship obtained after traversing the holes in the previous frame. If there is no corresponding hole in the previous frame that matches a hole in this frame, it suggests that the corresponding hole is newly generated, and a new number should be assigned according to the global number. If there is a corresponding hole in the previous frame that matches one of the holes in this frame, we then check the corresponding hole in the previous frame for the current frame. If it is the same hole, then there is a correct one-to-one match; otherwise, this frame's hole should be considered a new hole. Finally, if the hole in this frame matches multiple holes in the previous frame,



we need to examine the relationship between the area of each hole and the areas of the corresponding holes. If the two areas are close, it suggests that the hole has merged into multiple holes in the previous frame, and a new number should be assigned to this frame's hole. Otherwise, it suggests that there are multiple matching errors, and the closest hole should be assigned a new number, and the other holes should be assigned new numbers.

By utilizing the method described above, we can obtain the serial number of each hole, in which the number remains with the hole throughout its disappearance. This serial number enables us to monitor changes in the number of holes over time. We also obtain the current number of each hole in each frame, and further derive the time of the peak number of holes in one frame and the time when the number of holes reaches zero. These two values will serve as a basis for further analysis. Furthermore, by adding the serial number of each hole, certain regularities and statistical information for different life cycles of holes can be obtained. The above results can confirm the effectiveness of the Fire-MatteFormer method for the extraction and identification of the hole structure, which is further referred to in the analysis section.

### 3.2. Feature Analysis of Stabilization and Near-LBO Conditions

The stable and near-LBO flame structure images were obtained using a continuous 1 kHz OH-PLIF technique. The flame images sequences were processed via the Fire-MatteFormer method, and the entire generation and disappearance processes of hole features were acquired, as shown in Figure 4. In this section, we can record the number of holes existing in each image frame, the number of new holes generated, and thus obtain the change curves of the total number of holes and the change curve of the number of holes in each frame. In the stable combustion condition ( $\varphi = 0.4$ ), the hole structure (numbered  $H_2$ ) located in the flame arm zone takes about 4 ms to undergo the process from generation to disappearance. Meanwhile, the hole structure (numbered  $H_0$ ) located in the flame root zone emerges and disappears rapidly, which is mainly attributed to a reduced stretch extinction limit [32]. The hole structure information is of great significance in analyzing the mechanism of flame stability and excavating the inherent law of the interaction between the flow field and the combustion field. In the near-LBO combustion condition ( $\varphi = 0.1$ ), the number of the hole structure is small (less than  $30 \times 30$  pixels in a  $970 \times 1856$  image) and cannot continue to exist (it is unable to find the subsequent corresponding hole), indicating that the swirl flame becomes unstable at a low equivalence ratio level.

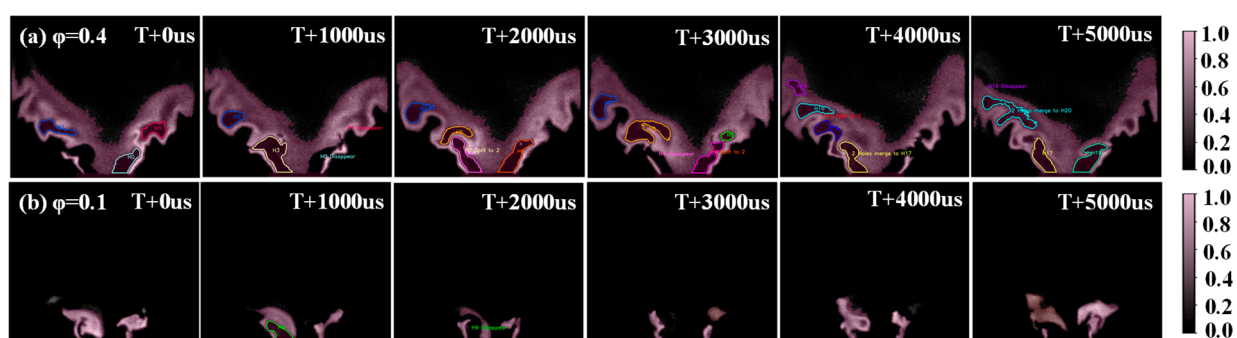


**Figure 4.** Selected 1 kHz OH-PLIF image sequences with hole feature markers. (a) Stable flame of  $\varphi = 0.4$ ; (b) near-LBO flame of  $\varphi = 0.1$ .

In addition, we also statistically analyze the regularity of the number of holes and the time interval between the peak number of holes and zero holes in each frame to explore the life cycle regularity of holes, as shown in Figure 5. We can clearly see the trend and change patterns of hole counts for both stabilization and near-LBO flames in 1000 frames. The following characteristics were found: In Figure 5a, the number of holes for near-LBO flames is much smaller than that of stable flames, and a comparison of slope results shows the growth trend of the hole number. Meanwhile, the number of holes generated by the

stable flame and the unstable flame at the current moment is described in Figure 5b. The hole number of the unstable flame at each moment is much smaller than the hole number of the stable flame, and it can be seen from the distribution density that the changes in the stable flame are more dramatic. Furthermore, Figure 5c explains the interval relationship between the moments when the number of adjacent holes is zero. It can be clearly seen that the interval between two holes with zero adjacent holes is clearer for a stable flame than for an unstable flame (period), which has an order of magnitude difference close to 102 times. Figure 5d represents the time intervals when the number of holes achieves the peak value, and it can be seen intuitively from the yellow line that if the number of vortices changes more violently, it is more unstable. The number of holes that appear at the 300th moment of a stable flame is the current peak value, and the interval difference is calculated after the 300th moment. If the number of holes appears after the 300th moment exceeds its peak, then the subsequent peak intervals are recalculated.

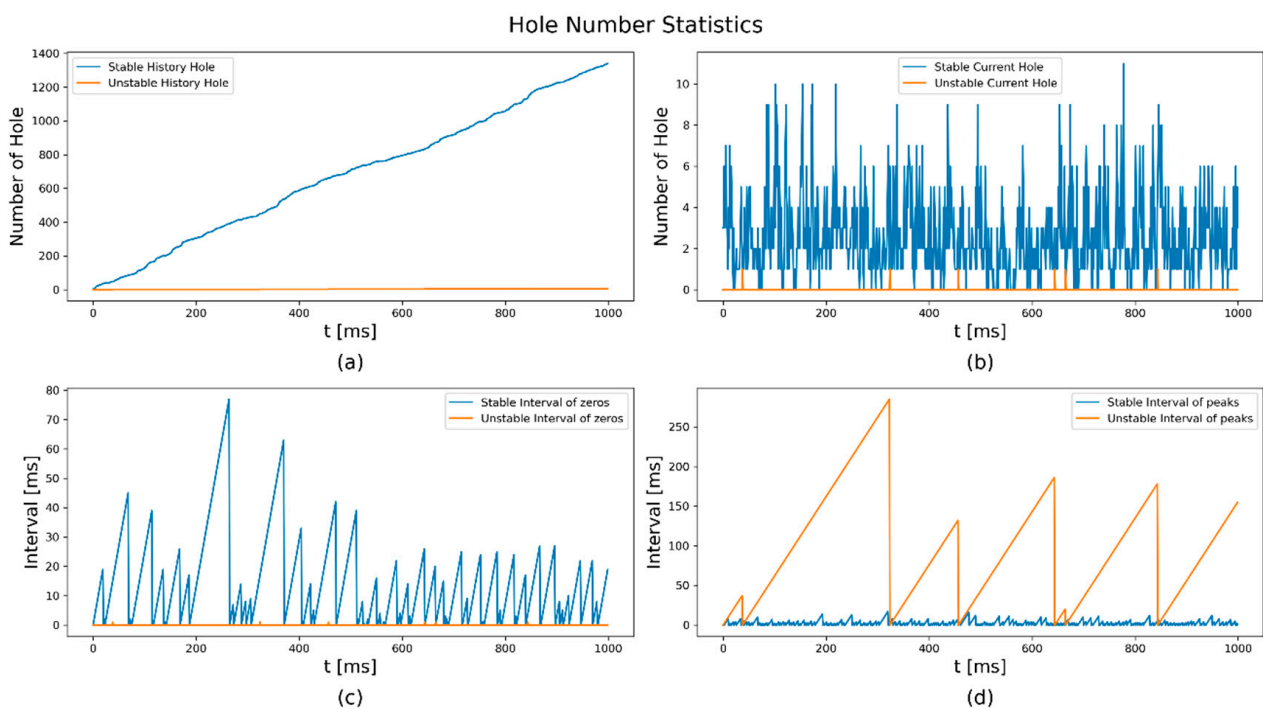


**Figure 5.** Statistical analysis results of hole numbers in stable and near-LBO flames. (a) The cumulative number of hole over time; (b) The existing number of the hole over time; (c) The interval after last zero (d) The interval after last peak.

As seen in the analysis results, firstly, there is a significant difference between stable and unstable flames. The number of holes is directly related to the stability of the flame. Stable flames can continuously produce holes, while unstable flames nearly produce holes. If the change from a stable flame to an unstable flame is continuous, the rate of hole production will decrease steadily in this process. Over time, the slope of the hole number curve will become smaller. Secondly, the average period of hole production from a stable flame is about 22.7 ms, which is the average period needed to generate zero in the hole count curve, which represents the average time to produce a hole during a cycle. After extracting the characteristic information of the hole according to the algorithm above, the circumference and area of each frame of the hole can be extracted. This means that the statistics and analysis of the entire test cycle can be carried out, and the life cycle of the hole (from the generation to the disappearance of the hole) can be calculated. The relationships between the full period and the hole area, circumference, and total number are expressed in the form of histogram and line graph. Figure 6 shows the hole life cycle and the total number of vortices in this cycle corresponding to the stable and near-LBO flames. A more

intuitive conclusion can be drawn: the area, quantity, circumference, and life cycle of the unstable flame in the hole are far inferior to those of the stable flame, and there is an order-of-magnitude gap. The statistical visualization research on the hole generation law can be intuitive and convenient for researchers to judge the stable flame and the unsteady flame intuitively and quickly, and, at the same time, it shows that the hole can be used as an important parameter to judge the combustion state of the flame.

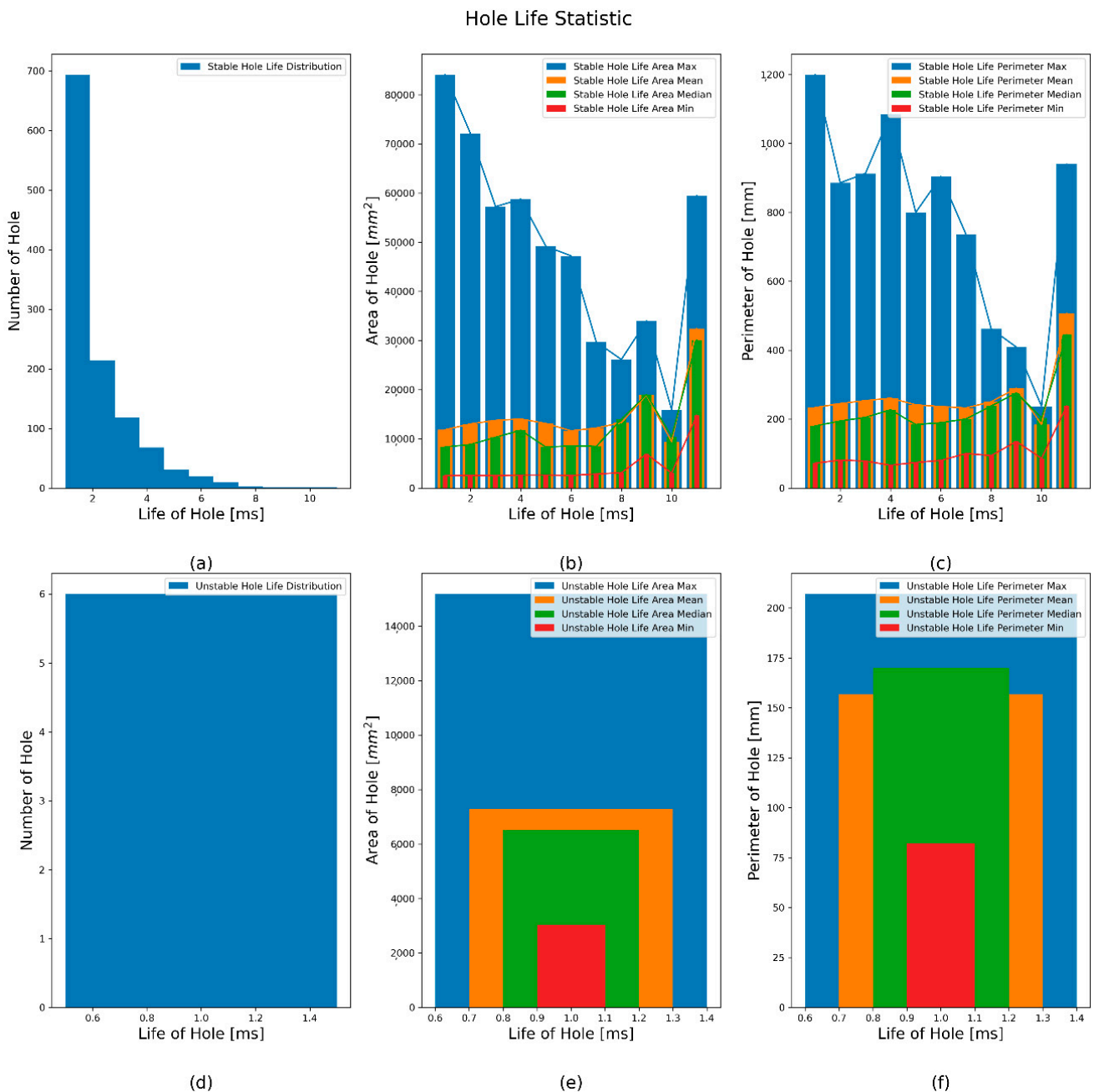


**Figure 6.** Statistical analysis results of hole lifecycle in stable and near-LBO flames. (a) Hole life distribution of stable flames; (b) Hole area distribution of stable flames; (c) Hole perimeter distribution of stable flames; (d) Hole life distribution of near-LBO flames; (e) Hole area distribution of near-LBO flames; (f) Hole perimeter distribution of near-LBO flames.

Finally, we ran the same algorithm to extract the characteristics of the hole through a new batch of flame data (01, 02, and 03) collected in the stable combustion environment, and conducted the same comparative experiment to generate a statistical map of the hole

characteristics. In Figure 7, we present the statistical line graphs of the flame hole of the three sequences together. In a new batch of different sequence data collected in the same environment, the change trend of the hole line conforms to the conclusion drawn in Figure 5. This further proves the effectiveness and versatility of our algorithm to extract the hole. The obtained local flame features can be used as important indicators of the LBO condition, which is significant in combustion model development and validation for both aero-engine and stationary gas turbine applications. Furthermore, the results can aid in establishing the feature fusion models for accurate prediction of the LBO condition, which solves the problem of engine reliance on pressure data to identify LBO accurately. The limitation of the current work mainly lies in the lack of richer LBO flame sample data. More flame data will improve the reliability of the model. In addition, flame state recognition work is not conducted online, but is obtained through offline analysis of data. In future, the proposed method and hole features are expected to aid in the development of new diagnostic tools, based on the field programmable gate array (FPGA), to achieve the online monitoring of the combustion condition. In addition, we will consider the combustion modes diagram to study the flame stabilization mechanism.

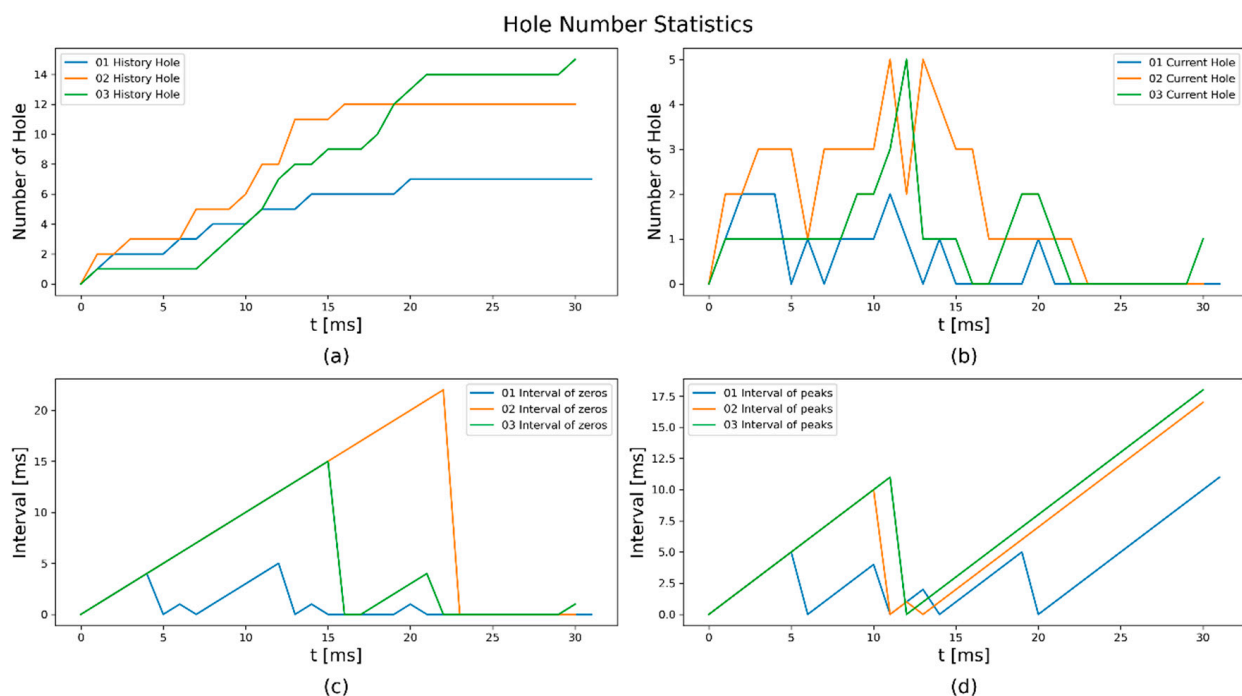


**Figure 7.** Statistical analysis results of hole number corresponding to the selected three sets of OH-PLIF image sequences. (a) The cumulative number of hole over time; (b) The existing number of the hole over time; (c) The interval after last zero; (d) The interval after last peak.

#### 4. Conclusions

In this paper, we propose a tri-map-based data-driven method to extract the local structure feature from high-speed OH-PLIF images. In order to achieve the early detection of near-LBO flame conditions, 10 kHz and 1 kHz OH-PLIF techniques were used to obtain the LBO flame motion to train and validate the model. This method utilizes an advanced neural network architecture to extract the main contour of flames from flame images and uses a series of post-processing steps to refine the contour. Finally, all flames and hole features in the flame images were extracted for further analysis. The hole features include the number of holes and the interval between the peak number values of the two holes. The generation and extinction of each hole were obtained to derive the life cycle of hole structures. Our results showed that the number of hole features was small and could not continue to exist in the near-LBO flame condition. The hole features were found to correlate

with the LBO flame condition, which might represent a novel precursor for the detection of incipient LBO instability conditions.

**Author Contributions:** Conceptualization, P.Y. and Z.C.; Methodology, J.P. and X.Y.; Validation, C.Y. and P.Q.; Formal analysis, S.Z. and M.H.; Resources, Z.C. and J.P.; Writing—Original Draft Preparation, P.Y.; Writing—Review and Editing, Z.C.; Data Curation, W.L. and Z.J. All authors have read and agreed to the published version of the manuscript.

**Funding:** This research was funded by the National Natural Science Foundation of China (Grant Nos. 62305087, 62175053); Heilongjiang Provincial Natural Science Foundation of China (Grant No. LH2021F028); Natural Scientific Research Innovation Foundation in Harbin Institute of Technology (Grant No. HIT.NSRIF202245).

**Data Availability Statement:** The data presented in this study are available on request from the corresponding author.

**Conflicts of Interest:** Author Zuo Jiang was employed by the company, China Aerospace Science and Industry Corporation. The remaining authors declare that the research was conducted in the absence of any commercial or financial relationships that could be construed as a potential conflict of interest.

## References

- Xu, L.; Zheng, J.; Wang, G.; Li, L.; Qi, F. Effects of swirler position on flame response and combustion instabilities. *Chin. J. Aeronaut.* **2022**, *35*, 345–355. [[CrossRef](#)]
- Ruan, C.; Chen, F.; Cai, W.; Qian, Y.; Yu, L.; Lu, X. Principles of non-intrusive diagnostic techniques and their applications for fundamental studies of combustion instabilities in gas turbine combustors: A brief review. *Aerosp. Sci. Technol.* **2019**, *84*, 585–603. [[CrossRef](#)]
- Zhao, Q.; Yang, J.; Liu, C.; Liu, F.; Wang, S.; Mu, Y.; Xu, G.; Zhu, J. Lean blowout characteristics of spray flame in a multi-swirl staged combustor under different fuel decreasing rates. *Chin. J. Aeronaut.* **2022**, *35*, 130–143. [[CrossRef](#)]
- Naitoh, T.; Okura, N.; Gotoh, T.; Kato, Y. On the evolution of hole rings with swirl. *Phys. Fluids* **2014**, *26*, 95–149. [[CrossRef](#)]
- Keeton, B.W.; Carpio, J.; Nomura, K.K.; Sánchezet, A.L.; Williams, F.A. Hole breakdown in variable-density gaseous swirling jets. *J. Fluid Mech.* **2022**, *936*, A21. [[CrossRef](#)]
- Wang, H.; Song, X.; Li, L.; Huang, H.; Sun, M. Lean blowoff behavior of cavity-stabilized flames in a supersonic combustor. *Aerosp. Sci. Technol.* **2021**, *109*, 106427. [[CrossRef](#)]
- Wang, Z.; Hu, B.; Deng, A.; Zhang, J.; Zhao, Q. Predicting lean blow-off of bluffbody stabilized flames based on Damköhler number. *Chin. J. Aeronaut.* **2019**, *32*, 98–113. [[CrossRef](#)]
- Doherty, L.O. Hole breakdown: A review. *Prog. Energy Combust. Sci.* **2001**, *27*, 431–481.
- Moise, P. Bistability of bubble and conical forms of hole breakdown in laminar swirling jets. *J. Fluid. Mech.* **2020**, *889*, A31. [[CrossRef](#)]
- Oberleithner, K.; Paschereit, C.; Seele, R.; Wygnanski, I. Formation of turbulent hole breakdown: Intermittency, criticality, and global instability. *AIAA J.* **2012**, *50*, 1437–1452. [[CrossRef](#)]
- Li, Z.S.; Li, B.; Sun, Z.W.; Bai, X.S.; Aldén, M. Turbulence and Combustion Interaction: High Resolution Local Flame Front Structure Visualization Using Simultaneous Single-shot PLIF Imaging of CH, OH, and CH<sub>2</sub>O in a Piloted Premixed Jet Flame. *Combust. Flame* **2010**, *157*, 1087–1096. [[CrossRef](#)]
- Sjoholm, J.; Rosell, J.; Li, B.; Richter, M.; Li, Z.; Bai, X.S.; Aldén, M. Simultaneous Visualization of OH, CH, CH<sub>2</sub>O and Toluene PLIF in a Methane Jet Flame with Varying Degrees of Turbulence. *Proc. Combust. Inst.* **2013**, *34*, 1475–1482. [[CrossRef](#)]
- Taamallah, S.; Shanbhogue, S.J.; Ghoniem, A.F. Turbulent flame stabilization modes in premixed swirl combustion: Physical mechanism and Karlovitz number-based criterion. *Combust. Flame* **2016**, *166*, 19–33. [[CrossRef](#)]
- Zhang, J.; Hui, X.; An, Q.; Steinberg, A.M. Transient dynamics of the precessing hole core in an intermittently shape-transitioning swirl flame. *Combust. Flame* **2023**, *250*, 112652. [[CrossRef](#)]
- Wang, S.; Zheng, J.; Xu, L.; An, Q.; Han, X.; Zhang, C.; Li, L.; Xia, X.; Qi, F. Experimental investigation of the helical mode in a stratified swirling flame. *Combust. Flame* **2022**, *244*, 112268. [[CrossRef](#)]
- Skiba, A.W.; Carter, C.D.; Hammack, S.D.; Miller, J.D.; Gord, J.R.; Driscoll, J.F. The influence of large eddies on the structure of turbulent premixed flames characterized with stereo-PIV and multi-species PLIF at 20 kHz. *Proc. Combust. Inst.* **2019**, *37*, 2477–2484. [[CrossRef](#)]
- Han, L.; Gao, Q.; Zhang, D.; Feng, Z.; Sun, Z.; Li, B.; Li, Z. Deep Neural Network-Based Generation of Planar CH Distribution through Flame Chemiluminescence in Premixed Turbulent Flame. *Energy AI* **2023**, *12*, 100221. [[CrossRef](#)]
- Oh, J.H.; Skiba, A.W.; Hammack, S.D.; Mitsingas, C.M.; Carter, C.D.; Lee, T. Temporally resolving premixed turbulent flame structures using self-supervised adversarial reconstruction of CH-PLIF. *Energy AI* **2023**, *11*, 100207. [[CrossRef](#)]
- Zhou, L.; Song, Y.; Ji, W.; Wei, H. Machine learning for combustion. *Energy AI* **2022**, *7*, 100128. [[CrossRef](#)]

20. Cao, Z.; Yu, X.; Peng, J.; Hu, B.; Wang, Z.; Yu, Y.; Gao, L.; Han, M.; Yuan, Y.; Wu, G. Flame features and oscillation characteristics in near-blowout swirl-stabilized flames using high-speed OH-PLIF and mode decomposition methods. *Chin. J. Aeronaut.* **2023**, *36*, 191–200. [[CrossRef](#)]
21. Gao, L.; Yu, X.; Peng, J.; Tian, Y.; Cao, Z.; Zhong, F.; Wu, G.; Han, M. Flame characteristics of a cavity-based scramjet combustor using OH-PLIF and feature extraction. *Int. J. Hydrog. Energy* **2022**, *47*, 20662–20675. [[CrossRef](#)]
22. Hasti, V.R.; Navarkar, A.; Gore, J.P. A data-driven approach using machine learning for early detection of the lean blowout. *Energy AI* **2021**, *5*, 100099. [[CrossRef](#)]
23. Roncancio, R.; Gamal, A.E.; Gore, J.P. Turbulent flame image classification using Convolutional Neural Networks. *Energy AI* **2022**, *10*, 100193. [[CrossRef](#)]
24. Xu, N.; Price, B.; Cohen, S.; Huang, T. Deep image matting. In Proceedings of the IEEE Conference on Computer Vision and Pattern Recognition, Honolulu, HI, USA, 21–26 July 2017; pp. 2970–2979.
25. Park, G.T.; Son, S.J.; Yoo, J.Y.; Kim, S.; Kwak, N. Matteformer: Transformer-based image matting via prior-tokens. In Proceedings of the IEEE/CVF Conference on Computer Vision and Pattern Recognition, New Orleans, LA, USA, 18–24 June 2022; pp. 11696–11706.
26. Ruzon, M.A.; Tomasi, C. Alpha estimation in natural images. In Proceedings of the IEEE Conference on Computer Vision and Pattern Recognition, Hilton Head Island, SC, USA, 13–15 June 2000; pp. 18–25.
27. Chuang, Y.Y.; Curless, B.; Salesin, D.H.; Szeliski, R. A bayesian approach to digital matting. In Proceedings of the 2001 IEEE Computer Society Conference on Computer Vision and Pattern Recognition, Kauai, HI, USA, 8–14 December 2001.
28. Chuang, Y.Y.; Agarwala, A.; Curless, B.; Salesin, D.H.; Szeliski, R. Video matting of complex scenes. In Proceedings of the 29th Annual Conference on Computer Graphics and Interactive Techniques, San Antonio, TX, USA, 21–26 July 2002; pp. 243–248.
29. Vaswani, A.; Shazeer, N.; Parmar, N.; Uszkoreit, J.; Jones, L.; Gomez, A.N.; Kaiser, L. Attention is all you need. In Proceedings of the 31st Conference on Neural Information Processing Systems, Long Beach, VA, USA, 4–9 December 2017; Volume 30.
30. Liu, Z.; Lin, Y.; Cao, Y.; Hu, H.; Wei, Y.; Zhang, Z.; Lin, S.; Guo, B. Swin transformer: Hierarchical vision transformer using shifted windows. In Proceedings of the IEEE/CVF International Conference on Computer Vision, Montreal, BC, Canada, 11–17 October 2021; pp. 10012–10022.
31. Suzuki, S. Topological structural analysis of digitized binary images by border following. *Comput. Vis. Graph. Image Process.* **1985**, *30*, 32–46. [[CrossRef](#)]
32. Schmid, P.J.; Li, L.; Juniper, M.P.; Pust, O. Applications of the dynamic mode decomposition. *Theor. Comput. Fluid Dyn.* **2011**, *25*, 249–259. [[CrossRef](#)]

**Disclaimer/Publisher’s Note:** The statements, opinions and data contained in all publications are solely those of the individual author(s) and contributor(s) and not of MDPI and/or the editor(s). MDPI and/or the editor(s) disclaim responsibility for any injury to people or property resulting from any ideas, methods, instructions or products referred to in the content.